Zeitschrift: Schweizerische mineralogische und petrographische Mitteilungen = Bulletin suisse de minéralogie et pétrographie

Band: 78 (1998)

Heft: 2

Artikel: Reactions between eclogite and peridotite : mantle refertilisation by subduction of oceanic crust

Autor: Yaxley, Gregory M. / Green, David H.

DOI: https://doi.org/10.5169/seals-59286

SCHWEIZ. MINERAL. PETROGR. MITT. 78, 243–255, 1998

Reactions between eclogite and peridotite: mantle refertilisation by subduction of oceanic crust

by *Gregory M. Yaxley*[1] and *David H. Green*[1]

Abstract

An experimental approach has been used to explore and constrain recent suggestions that the incorporation of previously subducted eclogite in upwelling mantle plumes results in distinctive magmatic provinces of high melt volume and high silica and iron content. We have studied the melting behaviour of coesite eclogite, crystallised from average altered oceanic crust composition (GA1), at a pressure of 3.5 GPa. This pressure was chosen as representing much thicker lithosphere than in mid-ocean ridge petrogenesis, and conditions well within the eclogite stability field.

The coesite eclogite solidus is at T ≤ 1250 °C and its liquidus is at T ≈ 1500 °C, compared with the MORB pyrolite (representing modern upper mantle) solidus at ≈ 1550 °C. Low degree partial melts are dacitic (> 63 wt% SiO_2, > 7 wt% alkalies) and co-exist with coesite eclogite residue. Higher temperature melts (T ≥ 1350 °C) move along the garnet-clinopyroxene cotectic, remaining andesitic to basaltic andesitic in composition and producing liquidus phases which converge towards compositions typical of garnet and clinopyroxene of mantle peridotite.

Interactions between siliceous partial melts of eclogite and peridotite were investigated by sandwiching a layer of GA1 against MORB pyrolite and conducting experiments at 3.5 GPa between the coesite eclogite solidus and the pyrolite melting interval. Experiments at 1200–1400 °C became melt free; the siliceous melt from the eclogite layer producing orthopyroxene enrichment in neighbouring lherzolite and leaving sub-solidus refractory garnet and clinopyroxene in the former eclogite layer. At higher temperatures (≥ 1425 °C) a nepheline-normative picritic melt is formed, representing melting at the olivine-orthopyroxene-clinopyroxene-garnet minimum in an enriched lherzolite composition. At high pressures, a thermal divide represented by pyrope-rich garnet, omphacite and orthopyroxene, divides the SiO_2-rich liquids from eclogite sources, from nepheline-normative picritic liquids in alkali-rich, lherzolitic sources. Liquids cannot mix through this thermal divide. The process of re-fertilisation of mantle by admixing of subducted crust is achieved by ephemeral melts from eclogite sources effecting local mineralogical change, particularly in orthopyroxene : olivine ratio. Residual phases from eclogite and metasomatised phases in lherzolite converge in composition, but modal inhomogeneity (bands, lenses and schlieren) is enhanced. Heating or adiabatic upwelling of this modally heterogeneous mantle produces nepheline-normative picritic liquids at the solidus, or tholeiitic picritic liquids at higher temperatures. Such liquids will be marginally higher than normal MORB in Fe/Mg at near solidus conditions, but are silica-poor and olivine-rich. Trace and minor element, and isotopic characteristics will reflect the pre-history of the admixed materials, the time-integrated variations reflecting modal variations and the proportions of the admixed material and "normal mantle".

Keywords: coesite eclogite, peridotite, melting experiments, partial melts, mantle refertilisation.

1. Introduction

A number of models for basalt petrogenesis have attributed both the erupted volume, and certain distinctive isotopic and trace element characteristics of some basalt provinces, to the presence of both eclogite and peridotite in the mantle source regions. Eclogite present in the peridotite-dominated mantle may be derived from the basaltic component of subducted oceanic lithosphere, recycled back into the convecting mantle on a timescale of 1–2 Ga (HOFMANN, 1997). On trace element and isotopic grounds, ancient recycled oceanic crust may constitute the "HIMU" component, one of several inferred mantle reservoirs in the source regions of some ocean island basalts and flood basalt provinces (CHRISTENSEN and HOFMANN, 1994; HOFMANN, 1997; HOFMANN and

[1] Research School of Earth Sciences, Australian National University, Canberra, ACT 0200, Australia. <Greg.Yaxley@anu.edu.au>

WHITE, 1982; CHASE, 1981; ZINDLER et al., 1982; RINGWOOD, 1982).

Whilst there is uncertainty in the nature and form of eclogitic bodies derived from entrainment of subducted oceanic crust and lithosphere into the convecting, peridotite-dominated mantle, it appears likely that they could exist as elongate streaks with thicknesses of metres to kilometres (ALLEGRE and TURCOTTE, 1986). Heating of such heterogeneous mantle may cause the eclogite to melt at lower temperatures than the surrounding peridotite. Similarly, if there is adiabatic ascent of the heterogeneous mantle in plumes or diapirs, eclogite would melt at greater depths than surrounding peridotite (YASUDA et al., 1994). Hence, there is potential for reactions and mixing processes between siliceous partial melts of eclogite, and lherzolitic mantle wall-rock. Our experimental investigation explores the nature of these reactions and mixing caused by source rock inhomogeneity during partial melting in the upper mantle.

2. Experimental approach

2.1. CHOICE AND PREPARATION OF COMPOSITIONS

Compositions used are presented in table 1, and include an average oceanic basalt (GA1; YAXLEY and GREEN, 1994), representing recycled oceanic crust, and MORB pyrolite (MPY90), a fertile mantle composition suitable as a MORB-source (GREEN et al., 1979).

Starting mixes with these compositions were prepared from synthetic high purity oxides and carbonates, which were mechanically ground to homogeneous, fine-grained powders under analytical grade acetone. Iron was added as Fe_2O_3 and synthetic fayalite in GA1, and as fayalite in MPY90. The mixes were fired overnight at 1000 °C to decompose carbonates, and to partially fuse and react components. Fayalite was blended under acetone after firing. Both mixes were dried for several hours at 400 °C in an Ar atmosphere, and thereafter stored at 110 °C, to ensure complete dryness.

Tab. 1 Compositions of GA1 and MPY90. Mg# = 100 · Mg/(Mg + ΣFe).

	GA1	MPY90
SiO_2	50.35	44.74
TiO_2	1.49	0.17
Al_2O_3	16.53	4.37
FeO	9.83	7.55
MnO	0.17	0.11
MgO	7.94	38.57
CaO	9.60	3.38
Na_2O	3.49	0.40
K_2O	0.44	0.00
P_2O_5	0.16	0.00
Cr_2O_3	0.00	0.45
NiO	0.00	0.26
Mg#	59.00	90.10

We have avoided the use of natural pyroxenes and garnet from high pressure pyroxenites or eclogites as starting materials, and we have also avoided the use of porous diamond aggregate as a means of attempting to determine melt compositions at low degrees of melting. Experience shows that these techniques, particularly in combination, produce disequilibrium melts from the crystalline starting materials run well outside their conditions of formation, pressure gradients within the diamond aggregate and persistence of relict mineral cores (FALLOON et al., 1997). Since we have deliberately engineered chemical gradients in our layered experiments, it was most important that the homogeneity and fine-grain size of glass or low pressure sintered oxide mixes were part of the experimental method.

2.2. EXPERIMENTAL TECHNIQUES

Nominally anhydrous experiments were conducted at 3.5 GPa and 1200–1550 °C in a standard 1.27 cm piston-cylinder apparatus. Samples were run in sealed graphite-lined Pt capsules, in order to prevent Fe-loss by contact between the samples and the Pt. The capsule assembly was surrounded by alumina tubes and discs, and placed between composite 60% dense MgO and/or pyrophyllite inserts (fired at 1050 °C). Graphite heaters were used in NaCl/pyrex sleeves.

In all experiments the sample assemblies were heated and pressurised simultaneously. Temperature was controlled by a Eurotherm 904 controller attached to a type B thermocouple ($Pt_6Rh_{94}/Pt_{30}Rh_{70}$), and is accurate to ± 10 °C and precise to ± 1 °C. No correction was made for the effect of pressure on thermocouple output emf. No frictional correction to pressure was necessary because of the use of NaCl sleeves. The hot piston-out technique was used, and pressures are accurate to ± 0.1 GPa. Experiments were quenched by terminating the power to the furnace.

We first established the phase relations and partial melt compositions of the basalt composition (GA1) at 3.5 GPa, and then ran a series of peridotite/basalt layered and homogeneously

Tab. 2 Run conditions and assemblages for GA1 melting experiments, GA1/MPY90 layered experiments, and the GA1/MPY90 homogenously mixed run. All runs were conducted at 3.5 GPa. The column headed "GA1 layer" refers to the assemblage which formed in the pre-run position of the GA1 layer, "Opx-rich layer" refers to the assemblage which crystallised adjacent to the former GA1 layer, and "garnet lherzolite layer" refers to the assemblage which crystallised within the former MPY90 layer, some distance from the GA1/MPY90 interface. Abbreviations are: ga = garnet, cpx = clinopyroxene, opx = orthopyroxene, ol = olivine, co = coesite, pic liq = picritic liquid, bas liq = basaltic liquid, bas-and liq = basaltic andesitic liquid, and liq = andesitic liquid, dac liq = dacitic liquid. See text for further descriptions of the distributions of phases in these runs.

Run No.	Temperature (°C)	wt% GA1	Time (hrs)	Assemblages GA1 layer	Opx-rich layer	Garnet lherzolite layer
GA1 melting runs						
9114	1500	100	5	bas liq	–	–
C383	1475	100	8	ga + cpx + bas-and liq	–	–
9014	1450	100	24	ga + cpx + bas-and liq	–	–
C321	1350	100	119	ga + cpx + and liq	–	–
9099	1300	100	168	co + ga + cpx + dac liq	–	–
C338	1250	100	164	co + ga + cpx + dac liq	–	–
GA1/MPY90 layered runs						
C270	1550	35.3	24	pic liq	opx + pic liq	opx + pic liq
C275	1550	17.6	25	pic liq	ol + opx + pic liq	ol + opx + pic liq
C296	1500	10	24	pic liq	ol + opx + pic liq	ol + opx + pic liq
C327	1425	12.3	47	pic liq	opx + cpx + ga + ol + pic liq	ol + opx + cpx + ga
C333	1300/1425	13.6	144/48	pic liq	opx + cpx + ga + ol + pic liq	ol + opx + cpx + ga
C334	1250/1425	12.3	144/48	pic liq	opx + cpx + ga + ol + pic liq	ol + opx + cpx + ga
C308	1400	6.1	48	ga + cpx	opx + cpx + ol + ga	ol + opx + cpx + ga
C328	1300	7.4	168	ga + cpx	opx + cpx + ol + ga	ol + opx + cpx + ga
9117	1300	45.9	96	ga + cpx + and liq/ga + cpx	opx + cpx + ol + ga	ol + opx + cpx + ga
C339	1250	12.1	144	ga + cpx	opx + cpx + ol + ga	ol + opx + cpx + ga
C341	1200	13.2	163	ga + cpx	opx + cpx + ol + ga	ol + opx + cpx + ga
GA1/MPY90 mixed run						
C520	1500	50	72	cpx + ga + pic liq	–	–

mixed experiments to investigate interactions between partially molten eclogite and peridotite. Proportions of MPY90 : GA1 varied and are reported in table 2. In most layered runs, the basaltic layer was positioned at the top of the capsule and was underlain by the peridotitic layer. Experimental conditions and resultant phase assemblages are also reported in table 2.

2.3. ANALYTICAL TECHNIQUES

Upon recovery from the high pressure assemblies, capsules were mounted whole in epoxy, and sectioned longitudinally. The exposed run products were subjected to vacuum impregnation by additional epoxy to preserve textural relationships as much as possible, and were then polished. Polished run products were examined by reflected light microscopy, and by scanning electron microscopy (SEM) and electronprobe microanalysis (EPMA), using a JEOL 6400 SEM fitted with a Link Energy Dispersive Detector (Electron Microscopy Unit, ANU). Analytical conditions were 15 kV accelerating voltage and 1 nA beam current. Phase and melt compositions are reported in tables 3–5, and are averages of multiple analyses of each phase, using a focussed, 2–3 μm diameter beam for crystalline phases, and (where possible) a broad beam for quenched liquids (glasses). Detection limits for minor elements are 0.10 wt% for K_2O, TiO_2 and MnO, 0.15 wt% for Na_2O and Cr_2O_3, and 0.25 wt% for P_2O_5.

3. Experimental results

3.1. GA1 MELTING EXPERIMENTS

Quenched melt was present in all GA1 runs. At 1250 and 1300 °C well equilibrated assemblages of garnet + clinopyroxene + coesite + highly siliceous melt were produced. At 1350, 1450 and 1475 °C the assemblages contained garnet + clinopyroxene + melt. A run at 1500 °C contained glass only, indicating that the GA1 composition

Tab. 3 Compositions of phases and liquids from the GA1 melting experiments. Also shown are the results of least squares calculations of the proportions of each phase and melt in each experiment, including residual sum of squares (Σr^2). "Calc'd T (°C)" is the run temperature calculated using the geothermometer of ELLIS and GREEN (1979) for Fe–Mg exchange between garnet and clinopyroxene.

	C338 1250 °C co + ga + cpx + liq	9099 1300 °C co + ga + cpx + liq	C321 1350 °C ga + cpx + liq	9104 1450 °C ga + cpx + liq	C383 1475 °C ga + cpx + liq
Garnet (%)	26.8	25.4	26.6	10.1	9.1
Cpx (%)	58.6	60.6	40.5	18.5	4.5
Glass (%)	13.4	13.2	33.0	71.4	86.4
Coesite (%)	1.2	0.8	0.0	0.0	0.0
Σr^2	0.19	0.10	0.27	0.18	0.47
Garnet					
SiO_2	39.4	39.6	40.0	40.6	40.9
TiO_2	1.2	1.0	0.9	1.0	0.7
Al_2O_3	21.9	22.1	22.3	22.2	23.1
FeO	18.7	18.5	16.5	13.8	12.5
MnO	0.4	0.4	0.5	0.4	0.3
MgO	10.7	10.9	12.2	14.3	15.1
CaO	7.3	7.0	7.5	7.5	7.2
Na_2O	0.1	0.1	0.1	0.1	0.0
K_2O	0.0	0.0	0.1	0.0	0.0
P_2O_5	0.3	0.3	0.1	0.1	0.2
Mg#	50.6	51.3	56.8	64.8	68.4
Clinopyroxene					
SiO_2	51.1	51.3	51.3	50.3	51.1
TiO_2	1.6	1.4	0.8	0.5	0.5
Al_2O_3	14.9	14.8	14.1	14.4	13.8
FeO	7.1	7.4	6.8	6.7	6.2
MnO	0.2	0.2	0.1	0.2	0.1
MgO	8.2	8.2	9.7	11.0	11.6
CaO	12.4	12.2	13.3	13.7	13.8
Na_2O	4.4	4.4	3.8	3.1	2.7
K_2O	0.0	0.1	0.0	0.0	0.1
P_2O_5	0.2	0.1	0.1	0.1	0.1
Mg#	67.2	66.4	71.9	74.4	77.1
Liquid					
SiO_2	64.7	63.2	57.9	51.6	51.6
TiO_2	2.7	3.0	2.8	1.9	1.5
Al_2O_3	14.7	14.7	15.1	16.2	16.2
FeO	4.2	4.9	8.4	10.3	9.8
MnO	0.0	0.1	0.1	0.1	0.2
MgO	1.4	1.0	2.2	6.0	6.9
CaO	3.9	4.0	7.5	9.2	9.8
Na_2O	4.1	4.3	4.5	3.7	3.2
K_2O	3.6	3.8	1.1	0.6	0.5
P_2O_5	0.8	0.9	0.4	0.3	0.3
Mg#	37.4	26.7	31.6	51.2	55.7
calc'd T(°C)	1297	1307	1296	1429	1432

was above its liquidus at this PT condition. Rutile was not observed in any run product.

Garnet grains were typically euhedral and up to 50 μm across (Fig. 1A). They were compositionally unzoned, and in runs at 1250 and 1300 °C, contained variable amounts of rounded coesite inclusions, and rarer tiny clinopyroxene inclusions. Mg# [where Mg# = 100 · atomic Mg/(Mg + ΣFe)] increased with temperature, from 50.6 at 1250 °C to 68.4 at 1475 °C. Grossular content did not vary systematically with temperature, but TiO_2 decreased from 1.15 at 1250 °C to 0.7 wt% at 1475 °C (Tab. 3).

Clinopyroxene grains (up to 20 μm long) were generally tabular and compositionally unzoned (Fig. 1A). They were omphacitic in composition, containing dominant diopsidic and jadeitic components. TiO_2 and Na_2O contents decreased with increasing temperature (Tab. 3). Application of the geothermometer for Fe–Mg exchange between garnet and clinopyroxene (ELLIS and GREEN, 1979) to phase compositions produced in these experiments generally reproduced run temperatures to within 50 °C, indicating an acceptably close approach to equilibrium during the experiments (Tab. 3).

In runs at 1250 and 1300 °C, rounded coesite grains (≈ 20 μm) were also present outside the garnet crystals and in contact with melt, garnet and clinopyroxene, but usually spatially associated with garnet grains (Fig. 1A).

In runs at 1250 and 1300 °C, melt quenched to tiny pools of glass (usually < 10 μm across) interstitial to residual phases, but significant growth of low Mg# metastable quench phases was not observed (Fig. 1A). The run at 1350 °C produced larger pools of glass containing acicular or feathery quench clinopyroxene crystals. At 1450 and 1475 °C, the degree of melting was sufficiently high such that isolated residual garnet and clinopyroxene grains were completely surrounded by quenched melt (dendritic or feathery Fe-rich clinopyroxene + glass).

The "liquid" compositions presented in table 3 are averages of a number of analyses of quenched pools and patches of glass and any included metastable quench phases, obtained using (where possible) a defocussed, broad electron beam (1 nA) in order to minimise (1) loss of volatile elements (particularly Na and K), and (2) the effect of any heterogeneities in quenched liquid compositions caused by growth of metastable phases during quenching. The measured compositions varied with temperature from dacitic (1250 and 1300 °C), through andesitic (1350 °C), to basaltic andesitic (1450 and 1475 °C). The liquids were rich in TiO_2 (1.5–3.0 wt%), P_2O_5 (0.28–0.86 wt%) and alkalies (3.2–4.5 wt% Na_2O; 0.45–3.8 wt% K_2O). K_2O, TiO_2 and P_2O_5 decreased systematically with increasing temperature over the interval from 1300 to 1500 °C. However, each of these oxides (and Na_2O) was slightly lower in abundance in the estimated liquid composition at 1250 °C compared with that at 1300 °C. Mg# increased from 26.7 to 55.6 from 1300–1500 °C but was higher in the 1250 °C liquid (Mg# = 37.4) than in the 1300 °C liquid (Fig. 2). The apparently anomalous nature of the 1250 °C melt composition may relate to the possibility of electron beam overlap on residual phases (low in Na, Ti and P, high Mg#) during EPMA of the small melt pools present in this run.

Liquid compositions derived from direct EPMA of glass and any included quench phases were checked for accuracy using least squares calculations of the form liquid + clinopyroxene + garnet ± coesite = GA1 bulk composition. In all cases, these calculations provided good fits with acceptably low residuals. Modal proportions of phases and melt are presented in table 3. The melt proportion increased systematically from 13.2 wt% at 1300 °C to 86.4 wt% at 1475 °C. The calculated melt fraction at 1250 °C was 13.4 wt%, although the actual value is presumably less than this, because of possible electron beam overlap on residual phases, as mentioned above. Proportions of residual phases decreased with increasing temperature (Tab. 3). Sandwich experiments would be required to establish the compositions of partial melts below 1300 °C (i.e.; < 13% melt), but are unnecessary for the purposes of this investigation.

3.2. GA1/MPY90 LAYERED EXPERIMENTS

Layered experiments produced complex, heterogeneous charges, with indications of substantial reaction between siliceous partial melts of the basaltic (now eclogitic) layer, and the peridotitic layer.

For example, four runs (C308, C328, C339 and C341) were conducted at 1200–1400 °C and contained ≈ 6–13 wt% GA1. In each case, a layer of fine-grained garnet + clinopyroxene crystallised in the pre-run position of the GA1 layer, and was in contact with a peridotitic layer dominated by large aluminous enstatite grains (up to 30 μm long), with subordinate olivine, garnet and clinopyroxene. This orthopyroxene-rich layer graded over a distance of 20 to 50 μm, into normal garnet lherzolite (typically 48% olivine + 25% orthopyroxene + 16% clinopyroxene + 11% garnet).

A further run containing approximately equal masses of GA1 and MPY90 was conducted at 3.5 GPa and 1300 °C (run 9117). The run product

was again heterogeneous with complex layering (Fig. 1B and C). The former GA1 layer constituted approximately half the volume of the charge, and was coesite-absent eclogite + dacitic glass. This layer changed abruptly to a ≈ 50 μm wide layer of melt-free garnet + clinopyroxene near the contact with peridotite. This layer was very similar in appearance to the garnet + clinopyroxene layers found in runs C308, C328, C339 and C341. Adjacent to this layer, was an orthopyroxene-dominated zone, which graded over ≈ 50 μm into garnet lherzolite.

The absence of residual coesite, and comparison of phase and melt compositions in the partially molten eclogite layer of run 9117 with those present in the GA1 melting experiments indicate a temperature somewhat higher than the nominal 1300 °C for run 9117. Fe–Mg partitioning between garnet and clinopyroxene is consistent with equilibration at 1360 °C (ELLIS and GREEN, 1979). Comparison of the degree of melting in the eclogitic layer of run 9117, calculated by mass balance (35 wt% glass + 22 wt% clinopyroxene + 43 wt% garnet), with that observed in the GA1 melting experiments implies that the actual run temperature was closer to 1350 °C than to 1300 °C. The reasons for this temperature discrepancy are unknown, but may relate to unusual heater deformation, or to incorrect positioning of the thermocouple bead during the run.

Three runs containing 12–14 wt% GA1 were conducted at 3.5 GPa and 1425 °C (C327, C333 and C334). In run C334, the layered experimental charge was first crystallised at 1250 °C for 144 hours, and was then ramped isobarically to 1425 °C for a further 48 hours. In run C333, the charge was first crystallised at 1300 °C for 144 hours, and was then also ramped isobarically to 1425 °C for 48 hours. Run C327 was brought directly to 1425 °C and held at this temperature for 47 hours (Tab. 2). The resultant assemblages were similar, consisting of a layer of picritic liquid, which had quenched to spinifex textured orthopyroxene and Fe-rich olivine with minor interstitial Fe-rich glass, in contact with a layer dominated by residual aluminous enstatite, with minor forsteritic olivine, pyropic garnet and sub-calcic clinopyroxene, and interstitial, quenched melt (Fig. 1D). In runs C327 and C334 coarse-grained orthopyroxene (up to 50 μm long) was the only observed phase in the 50–100 μm-wide zones immediately in contact with the quenched melt layer. In run C333, orthopyroxene, garnet and clinopyroxene were all present in contact with the picritic melt layer, although orthopyroxene was dominant. In all three 1425 °C runs, proportions of olivine, clinopyroxene and garnet increased, and the % of

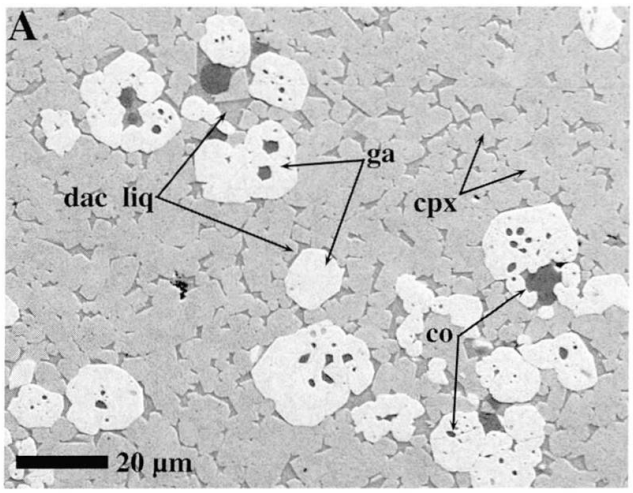

Fig. 1 Backscattered electron images of representative run products. (A) Run 9099, a GA1 melting run at 1300 °C, showing well-equilibrated assemblage of almandine-rich garnet (ga) + omphacitic clinopyroxene (cpx) + coesite (co) + quenched dacitic liquid (dac liq). (B) GA1/MPY90 layered run at 1300 °C (9117), run with approximately equal proportions of both starting compositions. The left hand side of the image (formerly GA1) consists of partially molten eclogite, and the right hand side of subsolidus garnet lherzolite. (C) A higher magnification view of the interface region of run 9117, showing the former GA1 layer which has crystallised as almandine-rich garnet (ga1) + omphacitic clinopyroxene (cpx1) + dacitic glass (dac liq), in contact with a melt-free layer of refractory garnet (ga2) + clinopyroxene (cpx2). This layer changes abruptly into a melt-free zone dominated by orthopyroxene (opx), with minor garnet (ga3), Fo_{87} olivine (ol) and clinopyroxene (cpx3), which grades into normal subsolidus garnet lherzolite over a distance of ≈ 50 μm. (D) GA1/MPY90 layered run at 1425 °C (C334), showing layer of picritic melt at the top of the capsule, in contact with a melt-bearing zone dominated by orthopyroxene, with minor olivine, which gradually grades into subsolidus garnet lherzolite near the bottom of the capsule. (E) GA1/MPY90 layered run at 1500 °C (C296), showing layer of picritic melt near the top of the capsule, and partially molten layer of orthopyroxene + olivine in the remainder of the charge.

interstitial melt and orthopyroxene decreased, with distance from the picritic melt layer. The orthopyroxene-rich, melt-bearing zone graded into a melt-absent region at the bottom of the capsule, consisting of a fine-grained assemblage of olivine > orthopyroxene > clinopyroxene > garnet (i.e.; garnet lherzolite). The total melt fraction in each of these runs was estimated using mass balance calculations to be ≈ 10%.

A run conducted at 1500 °C (C296) contained 10 wt% GA1 and 90 wt% MPY90. A picritic melt layer developed at the top of the capsule (Fig. 1E). The liquid had quenched to spinifex-textured orthopyroxene, minor clinopyroxene, olivine and

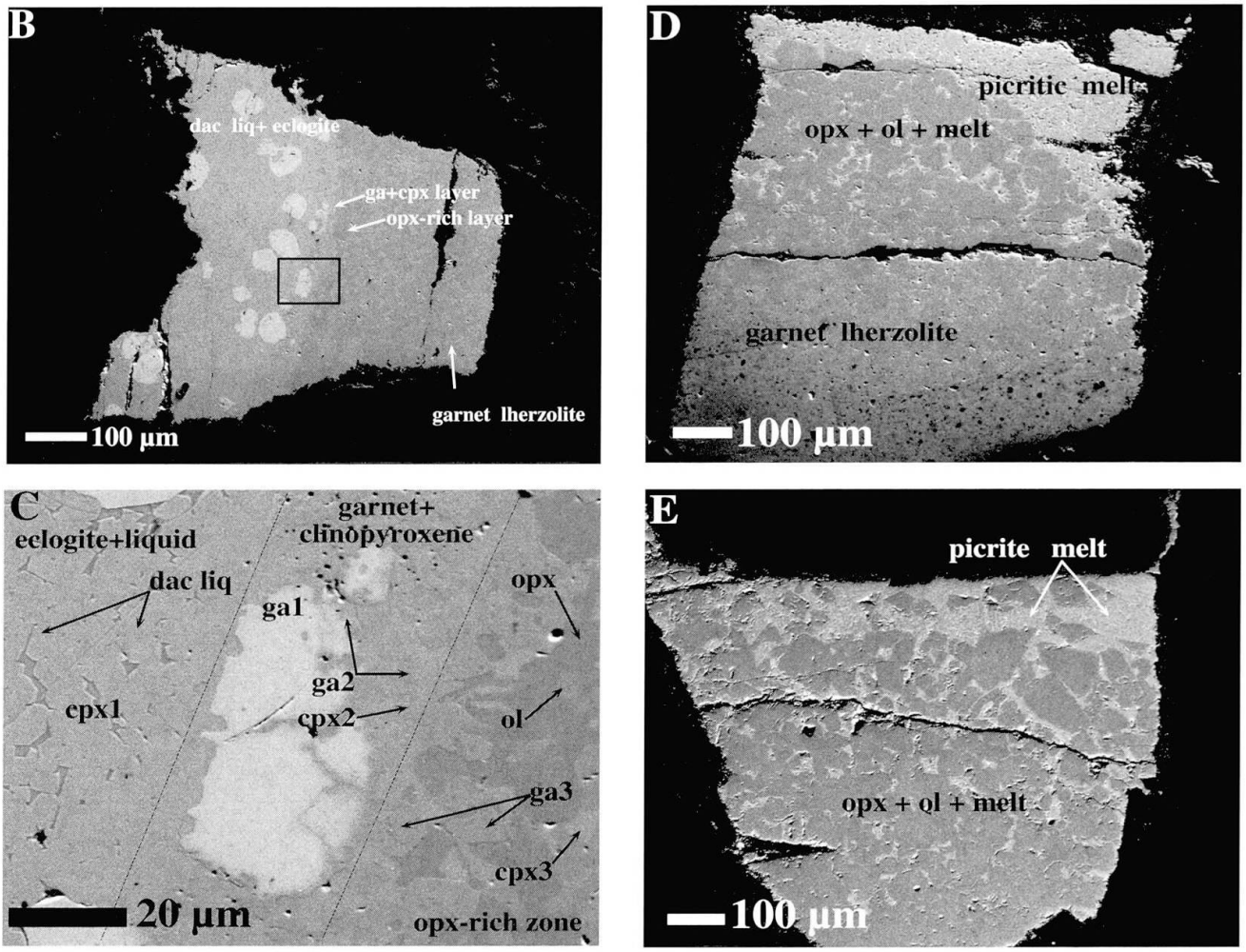

glass, and was in contact with well crystallised residual forsteritic olivine + aluminous enstatite + interstitial quenched melt, which extended throughout the remainder of the capsule. The proportion of melt decreased with distance from the picritic layer at the top of the capsules. In contrast to lower temperature runs, no garnet or clinopyroxene were detected.

Two runs (C275 and C270) were conducted at 1550 °C, containing 17.6 and 35.3 wt% GA1 respectively. C275 produced a layer of quenched picritic melt in contact with a layer comprised of coarse aluminous enstatite and olivine with interstitial quenched melt pools. Again, the proportion of melt decreased with distance from the picritic melt layer. C270 contained only picritic melt and coarse-grained residual aluminous enstatite.

Run C520 contained 50% each of GA1 and MPY90, homogeneously mixed, rather than layered. This was run at 3.5 GPa and 1500 °C, and produced sub-calcic clinopyroxene + garnet in equilibrium with picritic melt.

3.3. PHASE AND MELT COMPOSITIONS IN LAYERED AND MIXED EXPERIMENTS

In layered runs at T ≤ 1425 °C, olivines present in both the orthopyroxene-rich and the garnet lherzolite zones had similar Fo contents, indicating rapid diffusion and equilibration of Fe and Mg throughout the heterogeneous samples. Forsterite in olivine varied from 87.5 to 88.9 mol% in runs which contained no picritic melt (T ≤ 1400 °C), but was higher (88.9–90.7 mol%) in the 1425 °C runs, where ≈ 10% picritic melt was present. $Fo_{92.7}$ olivine occurred in runs C296 and C275 (1500 and 1550 °C respectively), coexisting with larger amounts (≈ 25%) of picritic melt.

Garnet was present in all layered runs at T ≤ 1425 °C, and in the homogeneously mixed run at 1500 °C (C520). Representative compositions are presented in table 4 and figure 2. Garnet from the partially molten coesite eclogite layer in layered run 9117 (1300 °C) was the most FeO- and CaO-rich (Mg# = 55.7; wt% CaO = 6.6), and Cr_2O_3-poor (no detectable Cr_2O_3) in all the layered or mixed

Tab. 4 Representative phase compositions from the GA1/MPY90 layered and mixed experiments. Abbreviations and symbols; ga + cpx refers to phases from the garnet + clinopyroxene layers in runs at T ≤ 1400 °C, ga lhz = phases from the garnet lherzolite zones of runs at T ≤ 1425 °C, eclogite = phases from the partially molten eclogite zone of run 9117, opx-rich = phases from the orthopyroxene-rich zones of runs at T ≤ 1425 °C, mixed = phases from the homogenously mixed run C520, opx ± ol + pic liq = phases from runs at T ≥ 1500 °C. The asterix indicates that although the nominal run temperature of 9117 was 1300 °C, the phase assemblage and compositions, and the degree of melt present in the eclogitic zone suggest that the true run temperature was ≈ 1350 °C.

Clinopyroxene	C339 1250 °C ga+cpx	C339 1250 °C ga lhz	C308 1400 °C ga+cpx	C308 1400 °C ga lhz	9117 1300 °C* eclogite	9117 1300 °C* ga+cpx	9117 1300 °C* ga lhz	C333 1425 °C ga lhz	C334 1425 °C ga lhz	C327 1425 °C ga lhz	C520 1500 °C mixed
SiO_2	53.5	53.9	52.2	53.9	49.9	53.4	51.5	53.2	53.5	53.0	54.3
TiO_2	0.4	0.4	0.7	0.4	1.0	0.4	0.4	0.2	0.3	0.2	0.2
Al_2O_3	5.8	5.7	8.4	5.9	14.6	5.7	5.9	5.4	5.9	5.8	6.2
FeO	4.5	4.2	4.7	5.5	7.6	5.2	5.0	5.0	5.5	5.0	6.6
MnO	0.2	0.2	0.1	0.0	0.2	0.1	0.1	0.2	0.1	0.1	0.1
MgO	19.1	19.0	19.3	23.1	9.0	19.1	19.2	23.3	23.9	22.9	24.5
CaO	13.0	13.4	12.2	9.2	12.0	14.5	13.4	9.3	8.2	9.8	6.8
Na_2O	2.2	2.2	1.7	1.2	3.8	1.3	1.2	3.2	1.1	0.9	1.0
K_2O	0.0	0.1	0.0	0.0	0.1	0.0	0.0	0.1	0.1	0.0	0.0
P_2O_5	0.0	0.2	0.0	0.1	0.1	0.0	0.0	0.1	0.0	0.0	0.0
Cr_2O_3	0.3	1.0	0.3	0.6	0.0	0.3	0.7	0.6	0.7	0.7	0.3
NiO	0.1	0.2	0.0	0.0	0.1	0.0	0.1	0.0	0.1	0.0	0.0
Mg#	88.4	88.9	87.9	88.3	68.0	86.7	87.2	89.3	88.6	89.1	86.8
Garnet	C339 1250 °C ga+cpx	C339 1250 °C ga lhz	C308 1400 °C ga+cpx	C308 1400 °C ga lhz	9117 1300 °C* eclogite	9117 1300 °C* ga+cpx	9117 1300 °C* ga lhz	C333 1425 °C ga lhz	C334 1425 °C ga lhz	C327 1425 °C ga lhz	C520 1500 °C mixed
SiO_2	41.4	42.2	40.2	43.0	39.5	42.3	41.5	42.1	41.7	42.2	42.7
TiO_2	0.6	0.6	1.3	0.6	0.9	0.7	0.5	0.5	0.4	0.4	0.5
Al_2O_3	23.1	21.9	22.3	23.1	22.1	23.2	22.2	23.0	21.5	22.7	23.0
FeO	9.7	7.3	13.2	6.9	17.0	8.5	7.2	7.0	6.7	6.4	7.7
MnO	0.4	0.3	0.3	0.2	0.5	0.2	0.0	0.3	0.1	0.1	0.1
MgO	18.5	21.8	15.4	21.8	12.0	19.9	20.0	21.9	22.1	22.3	21.4
CaO	5.4	4.6	6.3	4.8	6.6	5.3	5.1	4.8	4.4	4.6	4.2
Na_2O	0.0	0.0	0.0	0.0	0.0	0.0	0.0	0.0	0.0	0.0	0.0
K2O	0.0	0.0	0.0	0.0	0.0	0.0	0.1	0.1	0.0	0.1	0.1
P_2O_5	0.2	0.1	0.1	0.1	0.2	0.0	0.0	0.0	0.1	0.1	0.1
Cr_2O_3	0.1	1.2	0.0	1.6	0.0	0.4	1.3	1.4	1.3	1.5	0.5
NiO	0.0	0.0	0.0	0.0	0.1	0.0	0.0	0.2	0.1	0.0	0.0
Mg#	77.3	84.2	67.5	85.0	55.6	80.6	83.2	84.8	85.5	86.2	83.2
Orthopyroxene	C339 1250 °C opx-rich	C339 1250 °C ga lhz	C308 1400 °C opx-rich	C308 1400 °C ga lhz	9117 1300 °C* opx-rich	9117 1300 °C* ga lhz	C333 1425 °C opx-rich	C333 1425 °C ga lhz	C296 1500 °C opx+ol+ pic liq	C275 1550 °C opx+ol+ pic liq	C270 1550 °C opx+ pic liq
SiO_2	54.8	55.6	55.3	53.3	53.9	53.3	54.6	54.5	56.0	53.7	54.4
TiO_2	0.2	0.2	0.2	0.3	0.3	0.1	0.2	0.2	0.0	0.1	0.1
Al_2O_3	3.3	3.4	4.8	4.6	4.1	6.3	4.9	3.8	3.7	4.7	6.7
FeO	6.9	6.3	6.5	6.2	7.0	6.4	6.0	6.3	4.4	4.3	4.8
MnO	0.3	0.2	0.2	0.3	0.2	0.1	0.1	0.1	0.1	0.1	0.1
MgO	31.5	32.4	31.1	32.8	29.8	29.5	31.4	31.8	33.5	31.9	31.5
CaO	1.5	1.6	2.0	2.1	2.5	1.9	2.2	1.7	1.8	1.5	2.2
Na_2O	0.1	0.1	0.2	0.1	0.1	0.0	0.3	0.0	0.0	0.0	0.0
K_2O	0.0	0.0	0.0	0.0	0.0	0.0	0.0	0.2	0.0	0.0	0.0
P_2O_5	0.0	0.1	0.1	0.0	0.0	0.1	0.0	0.0	0.0	0.2	0.1
Cr_2O_3	0.2	0.5	0.4	0.5	0.1	0.7	0.5	0.4	0.4	0.4	0.4
NiO	0.1	0.0	0.0	0.1	0.1	0.0	0.1	0.0	0.0	0.0	0.0
Mg#	89.0	90.2	89.5	90.5	88.4	89.2	90.3	90.0	93.1	93.0	92.1

runs, and was most similar in composition to garnet from the 1350 °C eclogite melting run (C321). Garnets from the garnet lherzolite and orthopyroxene-rich regions of the layered runs at T ≤ 1425 °C were indistinguishable in composition within a single experiment, and contained 4.6–5.2 wt% CaO, 1.2–1.6 wt% Cr_2O_3, and had Mg# from 82.3–86.2. Garnet from the homogeneously mixed run was similar to that in the garnet lherzolite and orthopyroxene-rich zones of the layered runs at T ≤ 1425 °C. However, garnets from the garnet + clinopyroxene layers in runs at T ≤ 1400 °C had Mg#'s from 67.5 to 83.2, Cr_2O_3 < 0.4 wt%, and CaO from 5.3 to 6.3 wt%, and were intermediate in composition between garnet in garnet lherzolite and orthopyroxene-rich zones, and garnet in the eclogite melting experiments (Tab. 4, Fig. 2).

The data of table 4 and figure 2 illustrate very clearly the approach of garnet to homogenisation and equilibrium within an assemblage of olivine + orthopyroxene + clinopyroxene + garnet, in terms of the major elements Ca, Mg, Fe and Al, and incompatible elements such as Na and Ti at T ≥ 1300 °C. Thus, in figure 2, garnet from the original eclogite bands moves to lower grossular content as required for equilibrium with orthopyroxene and olivine. However, the refractory, or strongly compatible element Cr does not redistribute, reflecting its low solubility in the ephemeral dacitic

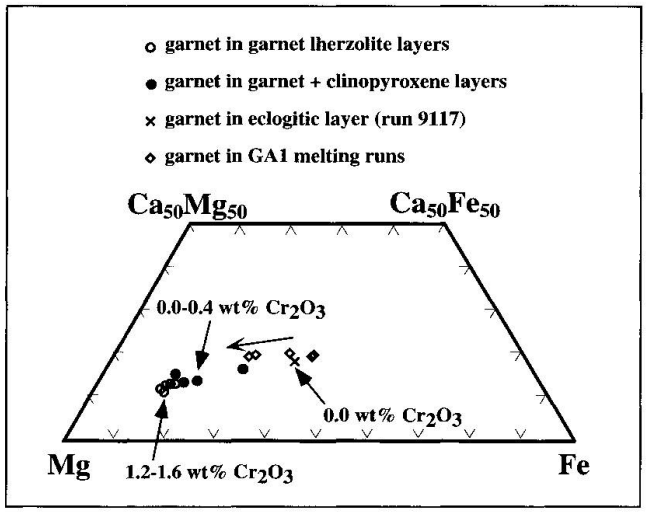

Fig. 2 Garnet compositions from GA1 melting runs, and from the garnet lherzolite zones and garnet + clinopyroxene zones from GA1/MPY90 layered runs at T ≤ 1425 °C, with range of Cr_2O_3 contents indicated. The arrow indicates the trend of garnet compositions with increasing temperature in the GA1 melting experiments. Note that garnets from the garnet + clinopyroxene zones of the layered runs are intermediate in composition to the eclogitic garnets from the GA1 melting runs, and the garnets from garnet lherzolite zones in the GA1/MPY90 layered runs. See text for further explanation.

or andesitic melts. To a lesser extent, NiO contents of phases in increasingly refractory eclogites or websterites are expected to remain low; up to the picrite solidus for the modified peridotite composition.

In the garnet lherzolite regions in runs at T ≤ 1400 °C (except 9117), clinopyroxene systematically decreased in CaO from 15.0 to 9.0 wt%, and coexisting orthopyroxenes systematically increased in CaO from 1.3–2.1 wt%, as temperature increased from 1200 to 1400 °C. Abundances of Al_2O_3 in clinopyroxenes from the garnet lherzolite regions in these runs were rather constant (mean = 5.7 wt%) (Tab. 4). Clinopyroxenes from the garnet + clinopyroxene layers in runs at T ≤ 1400 °C were similar or higher in Al_2O_3 (5.7–10.8 wt%), had 12.0–14.5 wt% CaO, and Mg#'s from 86.7–88.5. Non-systematic variation of phase compositions with increasing temperature, and the fact that calculations based on Fe–Mg exchange between garnet and clinopyroxene in the garnet + clinopyroxene layers did not accurately reproduce run temperatures, suggest lack of equilibration between phases in the garnet + clinopyroxene layers.

Orthopyroxene was present in all layered runs, in the orthopyroxene-rich zones adjacent to the garnet + clinopyroxene (T ≤ 1400 °C) or picritic melt (T = 1425 °C) layers, in the garnet lherzolite zones in runs at T ≤ 1425 °C, or as a residual phase to picritic melt in runs at T ≥ 1500 °C. In the garnet lherzolite zones, orthopyroxenes exhibited nearly constant Mg# (mean 90.1), Al_2O_3 from 2.9–6.3 wt%, and CaO from 1.3–2.1 wt% (Tab. 4). Orthopyroxenes in the orthopyroxene-rich zones were slightly more FeO-rich (mean Mg# = 89.6), but otherwise were very similar in composition to coexisting orthopyroxenes in garnet lherzolite zones. Orthopyroxenes from picritic melt-bearing runs at T ≥ 1500 °C had significantly higher Mg#'s (92.1–93.1), CaO from 1.5 to 2.2 wt%, and Al_2O_3 from 3.7 to 6.7 wt% (Tab. 4).

Compositions of liquids present in layered runs at T ≥ 1425 °C (Tab. 5) were estimated by averaging a number of broad beam electron-probe analyses of quenched melt layers. The melts were broadly picritic (MgO = 18.6–22.1 wt%) with Mg# from 74.8 to 81.5, and CaO/Al_2O_3 from 0.74 to 0.88. Melt from layered runs at 1425 °C (C334, C333 and C327) were richer in incompatible minor elements such as Na_2O, K_2O and TiO_2, but lower in SiO_2, MgO and Mg# than melts produced in layered runs at 1500 or 1550 °C. K_d for Fe–Mg partitioning between olivine (in any textural setting) and coexisting picritic liquid [$K_d = (Fe/Mg)_{ol}/(Fe/Mg)_{liq}$] varied between 0.30 and 0.36 for all picrite-bearing runs, suggesting a close

Tab. 5 Average compositions of picritic melts from layered and mixed runs at T ≥ 1425 °C. $K_d = [(FeO/MgO)_{ol}/(FeO/MgO)_{liq}]$.

	C334 1250/1425 °C	C333 1300/1425 °C	C327 1425 °C	C296 1500 °C	C520 1500 °C	C275 1550 °C	C270 1550 °C
SiO_2	46.3	44.7	44.9	48.2	45.9	46.9	46.8
TiO_2	1.4	1.4	1.5	0.5	1.8	0.9	1.0
Al_2O_3	11.1	11.3	10.6	9.9	11.7	11.4	11.6
FeO	10.3	11.2	11.6	8.9	12.5	9.3	8.9
MnO	0.1	0.1	0.1	0.1	0.2	0.2	0.2
MgO	18.6	18.7	19.2	22.1	16.5	20.8	20.6
CaO	9.2	9.4	9.4	8.5	8.4	8.9	8.6
Na_2O	2.0	1.9	2.0	1.1	2.1	1.2	1.7
K_2O	0.5	0.5	0.3	0.1	0.5	0.2	0.3
Cr_2O_3	0.2	0.3	0.3	0.4	0.2	0.3	0.2
P_2O_5	0.2	0.3	0.1	0.1	0.2	0.2	0.2
Mg#	76.3	74.8	74.6	81.5	70.2	80.0	80.5
K_d	0.36	0.32	0.30	0.35	–	0.32	–

approach to local Fe–Mg equilibrium between picritic melt and residual olivine throughout each capsule (ROEDDER and EMSLIE, 1970).

4. Discussion

4.1. MELTING PHASE RELATIONS IN THE GA1-MPY90 SYSTEM

In the following discussion we utilise a molecular normative projection to illustrate melting relations in the GA1 and MPY90 systems. We have projected the siliceous melts from the GA1 melting experiments, and the picritic melts from the layered and mixed experiments, into a molecular normative "high-pressure eclogite tetrahedron" $(Di + Jd)_{ss}$–Ol–Qz–Ga, where garnet is Gr_{50} $(Alm + Py)_{50}$ (Fig. 3). We assume that the picritic melts present in the layered runs at 1425 °C are in equilibrium with garnet lherzolite, as partial melting extends throughout the orthopyroxene-rich layer into the garnet lherzolite layer in these charges. Similarly, we assume that the picritic melts present in layered runs at T ≥ 1500 °C are saturated in the crystalline residues present, i.e.; aluminous enstatite ± forsteritic olivine.

Projections of the partial melt compositions onto the faces of this tetrahedron illustrate the large compositional separation between partial melts of eclogite, and the picritic melts in equilibrium with orthopyroxene ± olivine, or with garnet lherzolite phases in the layered experiments, or with clinopyroxene + garnet in the mixed run. The low degree partial melts of GA1 at 1250 and 1300 °C lie within a compositionally restricted field near the Qz apex, for dacitic or rhyodacitic minimum melts multiply saturated in coesite, clinopyroxene and garnet at 3.5 GPa. The higher degree partial melts of GA1 (T ≥ 1350 °C) lie along a cotectic, which is the intersection of liquidus phase fields for crystallisation of garnet and clinopyroxene. Similarly, the layered, melt-bearing experiments at 1425 °C define a field for picritic minimum melts saturated in garnet lherzolite phases. This field lies on the opposite side of the thermal divide (O'HARA, 1963 a and b; GREEN and RINGWOOD, 1968), close to the Ol apex, with orthopyroxene ± olivine ± melt-bearing layered runs at T ≥ 1500 °C, and the garnet + clinopyroxene + melt-bearing mixed run at 1500 °C, delineating cotectics between liquidus fields for crystallisation of olivine, orthopyroxene, and garnet. A partial melt composition of MPY90, in equilibrium with garnet lherzolite at 1600 °C (FALLOON and GREEN, 1988), also lies within the minimum melt field. This separation in compositions of low degree melts in the MPY90-GA1 system can be understood in terms of a high pressure thermal divide, expressed by the Hy – $(Di + Jd)_{ss}$ join in the projection from Ga onto the face $(Di + Jd)_{ss}$ – Qz – Ol (Fig. 3A), or by the Hy–Ga join in the projection from $(Di + Jd)_{ss}$ onto the face Ol–Qz–Ga (Fig. 3B).

The liquidus surfaces presented in figure 3 are schematic only. Further experimentation is required to precisely locate all phase boundaries within this compositional space.

4.2. INTERACTIONS BETWEEN PERIDOTITE AND PARTIALLY MOLTEN ECLOGITE

Subducted oceanic crust will convert to coesite eclogite at depths of ≈ 100 km (GREEN and RING-

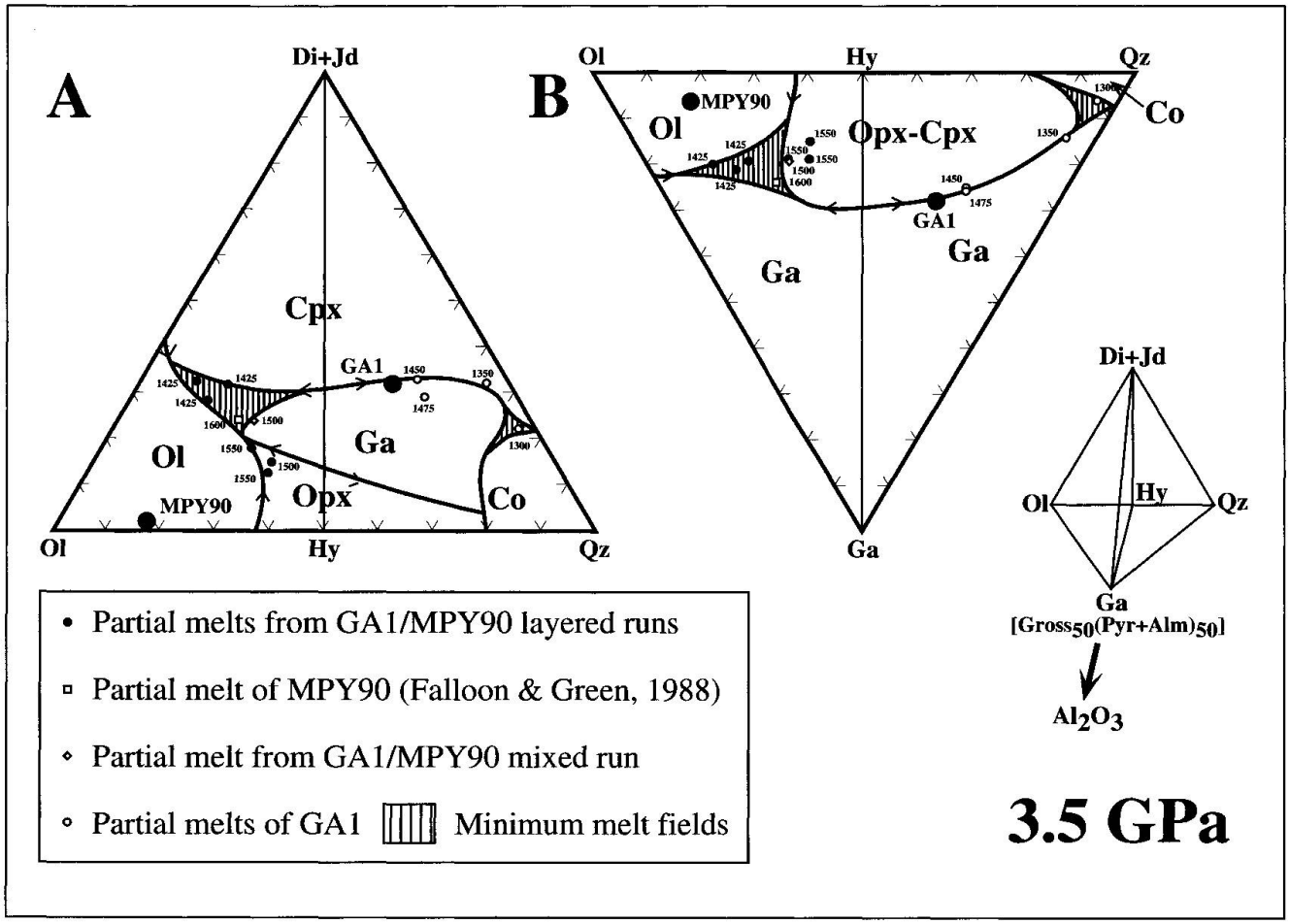

Fig. 3 Schematic liquidus phase relations at 3.5 GPa for GA1-MPY90 system. Melt compositions from the experiments are plotted as small symbols, with run temperatures indicated. Larger black dots represent the GA1 and MPY90 bulk compositions. Heavy black curves are approximate cotectics with arrows indicating down temperature direction. Fields for crystallisation of olivine (Ol), garnet (Ga), clinopyroxene (Cpx), orthopyroxene (Opx) and coesite (Co) are also indicated. Shaded areas are fields of minimum melting for GA1-rich bulk compositions (near Qz apex) and MPY90-rich bulk compositions (near Ol apex). (A) Projection from garnet (Ga) onto the face diopside + jadeite solid solution (Di + Jd) – olivine (Ol) – quartz (Qz). (B) Projection from (Di + Jd) onto the face Ol – Qz – Ga. The joins (Di + Jd) – Hy on (A) and Hy – Ga on (B) represent a thermal divide. See text for further explanation of the projections.

WOOD, 1967). This is expected to have a substantially lower solidus temperature than peridotite, at least within the upper mantle (YASUDA et al., 1994). As demonstrated above, near-solidus partial melts of eclogite are highly siliceous, and very reactive towards surrounding mantle peridotite. Migration of siliceous melts into peridotite will increase modal orthopyroxene in the wall-rock, and may result in formation of a body of bi-mineralic, refractory eclogitic residue, mantled by orthopyroxenite or orthopyroxene-enriched peridotite, with Mg# lower than normal mantle.

Further heating or adiabatic upwelling may induce further melting in the residual eclogite, which has lower Mg# and higher Na/Ca in clinopyroxene than the surrounding peridotite. These andesitic to basaltic andesitic partial melts will lie along the garnet-clinopyroxene cotectic in figure 3. If they migrate into the surrounding peridotite, they will also react, chiefly with olivine, increasing the proportions of garnet and pyroxene in peridotite, and moving garnet and clinopyroxene in the bi-mineralic eclogitic residue to more magnesian compositions. In this way, phase compositions in the eclogitic residue, and in the modified peridotite surrounding it, will tend to converge. However, phase *proportions* will remain distinctive, resulting in formation of bands and schlieren of orthopyroxene-enriched peridotite, websterite and garnet lherzolite. Similar mineralogical zoning has been described from many peridotite massifs, although this has generally been attributed to high pressure crystallisation of deeper-derived melts (e.g.; SUEN and FREY, 1987; BODINIER et al., 1987; BODINIER, 1988).

Because of the reaction processes described

above, partial melts of eclogite bodies entrained in peridotite in the upper mantle will be "ephemeral", in the sense that they will react out of existence within peridotite, and will be resorbed into sub-solidus mineral assemblages which lie on the garnet-pyroxene thermal divide, with mineral compositions trending towards homogeneity throughout the mixing zone.

Melting will next occur at the peridotite minimum (Fig. 3). If local heterogeneity in mineral compositions persists, then the "peridotite minimum" will vary in temperature and composition with mineral solid solution parameters, such as Na/Ca, Fe/Mg etc. Locally, because minerals have become slightly more Fe-rich and with higher Na/Ca in clinopyroxene than the phases of the model MPY90, melting will occur at lower temperatures than the solidus for MPY90, and preferentially on the margins of residual eclogite or pyroxenite against lherzolite (i.e.; where olivine + orthopyroxene + clinopyroxene + garnet are co-located). Partial melts will be strongly nepheline normative picrites, which will react with more refractory MPY90, enriching it in garnet and clinopyroxene. This process of local melting and redistribution will further homogenise the compositions of the mantle minerals. Local residues from picritic melt extraction will lie on the harzburgite, garnet harzburgite or garnet websterite cotectics on the schematic phase diagram in figure 3.

Continued heating or adiabatic ascent may enable continuation of such redistribution, until the originally basaltic component has reacted back into the garnet lherzolite mineralogy, producing modified peridotite with a bulk composition determined by the original proportions of basalt to peridotite. Further melting at high pressures, of this partially or completely homogenised, modified peridotite, will produce liquids of picritic or basaltic composition, whose major, minor and trace element abundances are controlled by bulk composition and by garnet lherzolite or harzburgite melting phase relations. The isotopic signatures of these melts will reflect their originally heterogeneous source histories.

5. Conclusions

1. The results described above preclude the possibility of direct mixing of partial melts of eclogite (siliceous melts) with partial melts of peridotites (picrites or basalts) in the mantle in order to enhance melt production and to produce melt compositions which are more siliceous and Fe-rich than MORB, as has been proposed for some continental flood basalts (CORDERY et al., 1997; CAMPBELL, 1997). Siliceous partial melts of eclogite are ephemeral in mantle plumes or diapirs and react with sub-solidus peridotite producing enrichment in orthopyroxene and modal heterogeneity in olivine, orthopyroxene, garnet and clinopyroxene. Melting processes will drive original eclogite phase compositions towards refractory garnet and clinopyroxene, approaching the compositions of garnet and clinopyroxene of the enclosing lherzolite. Refractory or strongly compatible minor or trace elements, particularly Cr or Ni, may remain inhomogeneously distributed, reflecting the earlier, greater heterogeneity.

2. The high pressure pyroxene-garnet thermal divide dominates melting relations in the peridotite-basalt system, and confines partial melts of the mantle to be picritic, or more olivine-rich liquid compositions, at pressures > 3 GPa. Subducted oceanic crust evolves from inhomogeneity in mineral modes and compositions (coesite eclogite in garnet lherzolite) towards compositional homogeneity in minerals, but contrasting modal abundances (bands, lenses and schlieren of orthopyroxenite, garnet websterite etc.).

3. Partial melts of the modally inhomogeneous source will be picritic and nepheline normative at near solidus conditions.

Acknowledgements

We gratefully acknowledge the technical assistance of Bill Hibberson (Research School of Earth Sciences, ANU), and Frank Brink and David Vowles (Electron Microscopy Unit, ANU). The manuscript benefitted from careful reviews by Drs O. Müntener and M. Ducea.

References

ALLÈGRE, C.J. and TURCOTTE, D.L. (1986): Implications of a two-component marble-cake mantle. Nature, 323, 123–127.

BODINIER, J.L. (1988): Geochemistry and petrogenesis of the Lanzo peridotite body, western Alps. Tectonophys., 149, 67–88.

BODINIER, J.L., GUIRAUD, M., FABRIES, J., DOSTAL, J. and DUPUY, C. (1987): Petrogenesis of layered pyroxenites from the Lherz, Freychinede and Prades ultramafic bodies (Ariege, French Pyrénées). Geochim. Cosmochim. Acta, 51, 279–290.

CAMPBELL, I.H. (1997): The mantle's chemical structure: Insights from the melting products of mantle plumes. In: JACKSON, I. (ed.): The Earth's Mantle: Composition, Structure and Evolution. Cambridge University Press, 259–310.

CHASE, C.G. (1981): Oceanic island Pb: Two-stage histories and mantle evolution. Earth Planet. Sci. Lett., 52, 277–284.

CHRISTENSEN, U.R. and HOFMANN, A.W. (1994): Segregation of subducted oceanic crust in the convecting mantle. J. Geophys. Res., 99, 19867–19884.

CORDERY, M.J., DAVIES, G.F. and CAMPBELL, I.H. (1997): Genesis of flood basalts from eclogite-bearing mantle plumes. J. Geophys. Res., 102, 20179–20198.

ELLIS, D.J. and GREEN, D.H. (1979): An experimental study of the effect of Ca upon garnet-clinopyroxene Fe–Mg exchange equilibria. Contrib. Mineral. and Petrol., 71, 13–22.

FALLOON, T.J. and GREEN, D.H. (1988): Anhydrous partial melting of peridotite from 8 to 35 kb and the petrogenesis of MORB. Special Lithosphere Issue, J. Petrol., 379–414.

FALLOON, T.J., GREEN, D.H., O'NEILL, H.ST.C. and HIBBERSON, W.O. (1997): The nature of near-solidus peridotite melts at 1 GPa. Earth Planet. Sci. Lett. (submitted).

GREEN, D.H. and RINGWOOD A.E. (1967): The genesis of basaltic magmas. Contrib. Mineral. Petrol., 15, 103–190.

GREEN, T.H. and RINGWOOD, A.E. (1968): Genesis of the calc-alkaline igneous rock suite. Contrib. Mineral. Petrol., 18. 105–162.

GREEN, D.H., HIBBERSON, W.O. and JACQUES A.L. (1979): Petrogenesis of mid-ocean ridge basalts. In: MCELHINNY, M.W. (ed.): The Earth: its origin, structure and evolution. Academic Press, London, 265–299.

HOFMANN, A.W. (1997): Mantle geochemistry: the message from oceanic volcanism. Nature, 385, 219–229.

HOFMANN, A.W. and WHITE, W.M. (1982): Mantle plumes from ancient oceanic crust. Earth Planet. Sci. Lett., 57, 421–436.

O'HARA, M.J. (1963a): Melting of garnet peridotite at 30 kilobars. Carnegie Inst. Wash. Year Book, 62, 71–76.

O'HARA, M.J. (1963b): Melting of bimineralic eclogite at 30 kilobars. Carnegie Inst. Wash. Year Book, 62, 76–77.

RINGWOOD, A.E. (1982): Phase transformations and differentiation in subducted lithosphere: Implications for mantle dynamics, basalt petrogenesis, and crustal evolution. J. Geology, 90, 611–643.

ROEDER, P.L. and EMSLIE, R.F. (1970): Olivine-liquid equilibrium. Contrib. Mineral. Petrol., 29, 275–289.

SUEN, C.J. and FREY, F.A. (1987): Origins of the mafic and ultramafic rocks in the Ronda peridotite. Earth Planet. Sci. Lett., 85, 183–202.

YASUDA, A., FUJII, T. and KURITA, K. (1994): Melting phase relations of an anhydrous mid-ocean ridge basalt from 3 to 20 GPa: implications for the behaviour of subducted oceanic crust in the mantle. J. Geophys. Res., 99, 9401–9414.

YAXLEY, G.M. and GREEN, D.H. (1994): Experimental demonstration of refractory carbonate-bearing eclogite and siliceous melt in the subduction regime. Earth Planet. Sci. Lett., 128, 313–325.

ZINDLER, A., JAGOUTZ, E. and GOLDSTEIN, S. (1982): Nd, Sr and Pb isotopic systematics in a three component mantle: A new perspective. Nature, 298, 519–523.

Manuscript received September 8, 1997; revision accepted March 17, 1998.